
Relating Cascaded Random Forests to Deep Convolutional Neural Networks for Semantic Segmentation

David L Richmond¹, Dagmar Kainmueller¹, Michael Y Yang²,
Eugene W Myers¹, and Carsten Rother²

¹MPI-CBG, ²TU Dresden
richmond@mpi-cbg.de

Abstract

We consider the task of pixel-wise semantic segmentation given a small set of labelled training images. Among two of the most popular techniques to address this task are Random Forests (RF) and Neural Networks (NN). The main contribution of this work is to explore the relationship between two special forms of these techniques: cascaded RFs and deep Convolutional Neural Networks (CNN). We show that there exists an (approximate) mapping from cascaded RF to deep CNN, and back. This insight gives two major practical benefits: a) the performance of a greedily trained cascaded RF can be improved; b) a deep CNN can be intelligently constructed and initialized. Furthermore, the resulting CNN architecture has not yet been explored for pixel-wise semantic labelling. We experimentally verify these practical benefits for the task of densely labelling segments of the developing zebrafish body plan in microscopy images.

1 Introduction

A central challenge in computer vision is the assignment of a semantic class label to every pixel in the image, a process known as semantic segmentation. A common strategy for semantic segmentation is to use pixel-level classifiers such as Random Forests (RF) [4], which have the advantage of being easy to train and performing well on a wide range of tasks, even in the face of little training data. The use of stacked classifiers, such as in Auto-context [27], has been shown to improve performance on many tasks such as object-class segmentation [25], facade segmentation [12], and brain segmentation [27]. However, this strategy has the limitation that the individual classifiers are trained greedily.

Recently, numerous groups have explored the use of Convolutional Neural Networks (CNNs) for semantic segmentation [7, 17, 6, 29], which has the advantage that it enables “end-to-end learning” of all model parameters. This trend is largely inspired by the success of deep CNNs on high-level computer vision tasks, such as image classification [14] and object detection [11]. However, deep CNNs require substantial experience and large labeled data sets to train [2, 3]. Thus, there currently exists a divide between cascaded classifiers, which perform well on semantic segmentation and can be trained with limited labelled data, and deep CNNs, which have recently been adapted to this task, and can dominate performance given enough training data.

Here, we propose an intermediate solution, exploiting the fundamental connection between decision trees (DT) and NNs [24] to bridge the gap between cascaded classifiers and deep CNNs. This provides a novel approach with the strengths of cascaded classifiers, namely robustness to limited training data, and the end-end-learning capacity of neural networks.

Contribution. Building upon the works of Sethi [24] and Welbl [28], we demonstrate that a cascaded RF is a special case of a deep CNN, with many sparse convolution kernels. To this end we describe a

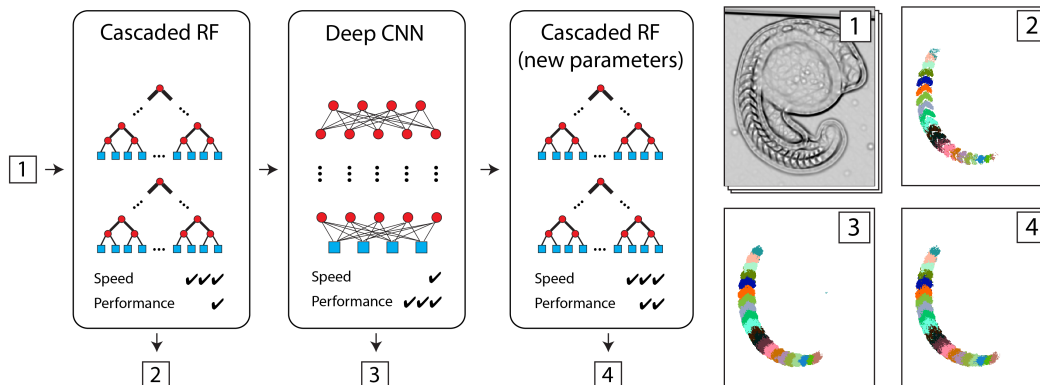


Figure 1: **Overview.** (Left box) A cascaded RF is trained to predict dense semantic labels. (Second left box) The cascaded RF is then mapped to a deep CNN and further trained to improve performance. (Third left box) Finally, the CNN is mapped back to a cascaded RF with updated parameters, for improved speed at test time with a slight reduction in performance. (Right) Application of the three classifiers to semantic segmentation of developing somites in microscopy images of zebrafish: Input filter stack (1) and corresponding output of the classifiers (2-4).

mapping to construct and initialize a CNN from a greedily trained RF cascade. This mapping enables effective end-to-end learning given limited training data. Furthermore, we derive an algorithm for mapping the CNN back to a cascaded RF for efficient test-time inference. As a proof-of-concept evaluation, we apply our method to biomedical data, where limited training data is a common problem. We focus on the challenging task of identifying and segmenting many self-similar structures, which requires strong contextual information for accurate labeling. For this, we chose semantic segmentation of 21 somites¹ in microscopy images of zebrafish embryos. We demonstrate that end-to-end training in the CNN improves segmentation accuracy, and we visualize the intermediate layers of the CNN to glean insights on its behavior. Figure 1 depicts our proposed pipeline.

2 Related Work

Our work relates to (i) global optimization of RF classifiers, (ii) mapping RF classifiers to neural networks, (iii) feature learning in cascaded RF models, (iv) applying CNNs to the task of semantic segmentation, and (v) training CNNs with limited labeled data. We cover each of these areas in turn.

Global Optimization of Random Forests. The limitations of traditional greedy RF construction [4] have been addressed by numerous works. In [26], the authors learn a DT by the standard greedy construction, followed by a process they call “fuzzification”, replacing all threshold split decisions with smooth sigmoid functions that they interpret as partial or “fuzzy” inheritance by the daughter nodes. They develop a back-propagation algorithm, which begins in the leaves and propagates up one layer at a time to the root node, re-optimizing all split parameters of the DT. In [21], they learn to combine the predictions from each DT so that the complementary information between multiple trees is optimally exploited. They identify a suitable loss function, and after training a standard RF, they retrain the distributions stored in the leaves, and prune the DTs to accomplish compression and avoid overfitting. However, [21] does not retrain the parameters of the internal split nodes of individual DTs, whereas [26] does not retrain the combination of trees in the forest.

Mapping Random Forests to Neural Networks. In both [26] and [21], RFs were initially trained in a greedy fashion, and then later refined. An alternative but related approach is to map the greedily trained RF to an NN with two hidden layers, and use this as a smart initialization for subsequent parameter refinement by back-propagation [24, 28]. This effectively “fuzzifies” threshold split decisions, and simultaneously enables training with respect to a final loss function on the output of the NN. Hence as opposed to [26] and [21], all model parameters are learned simultaneously in an end-to-end fashion. Additional advantages are that (i) back-propagation has been widely studied in

¹Somites are the metameric units that give rise to muscle and bone, including vertebrae.

this form, and (ii) back-propagation is highly parallelized, and only needs to propagate over 2 hidden layers, compared to all tree levels as in [26].

Our work builds upon [24, 28]: We extend their approach to a deep CNN, inspired by the Auto-context algorithm [27], for the purpose of semantic segmentation. Furthermore, we propose an approximate algorithm for mapping the trained CNN back to a RF with axis-aligned threshold split functions, for fast inference at test time.

Feature Learning in a Random Forest Framework. The Auto-context algorithm [27] attempts to capture pixel interdependencies in the learning process by iteratively learning a pixel-wise classifier, using the prediction of nearby pixels from the previous iteration as features. This process is closely related to feature learning, due to the introduction of new features during the learning process. Numerous works have generalized the initial approach of Auto-context. In Entangled Random Forests (ERFs) [18], spatial dependencies are captured by “entanglement features” in each DT, without the need for cascading. Geodesic Forests [13] additionally introduce image-aware geodesic smoothing to the class distributions, to be used as features by deeper nodes in the DT. However, despite the fact that ERFs use a *soft* sigmoid split function to obtain max-margin behaviour with a small number of trees, these approaches are still limited by greedy parameter optimization.

In a more traditional approach to feature learning, Neural Decision Forests [5] mix RFs and NNs by using multi-layer perceptrons (MLP) as soft split functions, to jointly tackle the problem of data representation and discriminative learning. This approach can obtain superior results with smaller trees, at the cost of more complicated split functions. However, the MLPs in each split node are trained independently of each other.

Here, we adopt the Auto-context algorithm for initial greedy feature selection in an RF cascade, which is subsequently trained end-to-end by back-propagation in the corresponding deep CNN.

Convolutional Neural Networks for Semantic Segmentation. While CNNs have proven very successful for high-level vision tasks, such as image classification, they are less popular for the task of dense semantic segmentation, due to their in-built spatial invariance. CNNs can be applied in a tile-based manner [7]; however, this leads to pixel-independent predictions, which require additional measures to ensure spatial consistency [10, 19]. In [17], the authors extend the tile-based approach to “whole-image-at-a-time” processing, in their Fully Convolutional Network (FCN). They address the coarse-graining effect of the CNN by upsampling the feature maps in deconvolution layers, and combining fine-grained and coarse-grained features during prediction. This approach, combining down-sampling with subsequent up-sampling, is necessary to maintain a large receptive field without increasing the size of the convolution kernels, which otherwise become difficult to learn. In [6], they minimize coarse-graining by skipping multiple sub-sampling layers and avoid introducing additional parameters by using sparse convolutional kernels in the layers with large receptive fields. They additionally post-process by a fully connected CRF. In [29], they address coarse-graining by expressing a mean-field CRF as a Recursive Neural Network (RNN), and concatenating this RNN behind a FCN, for end-to-end training of all parameters. Notably, they demonstrate a significant boost in performance on the Pascal VOC 2012 segmentation benchmark.

In our work we propose a new CNN architecture for semantic segmentation. Contrary to the previous approaches, we avoid coarse-graining effects, which arise in large part due to pre-training a CNN for *image classification* on data provided by the ImageNet Large Scale Visual Recognition Challenge (ILSVRC). Instead, we pre-train a cascaded RF on a small set of densely labeled data. Our approach is related to the use of sparse kernels in [6]; however, we learn the non-zero element(s) of very sparse convolutional kernels during greedy construction of an RF cascade. One advantage of our approach is that the sparsity of the kernels can be specified by the number of features used in each RF split node, independently of the size of the receptive field.

Training Neural Networks with Limited Labelled Data. CNNs provide a powerful tool for feature learning; however, their performance relies on a large set of labeled training data. Unsupervised pre-training has been used successfully to leverage small labeled training sets [23, 20]; however, fully supervised training on large data sets still gives higher performance. Alternatively, transfer learning makes use of *e.g.*, pseudo-tasks [1], or surrogate training data [8]. More recent practice is to train a CNN on a large training set, and then fine tune the parameters on the target data [11]. However, this requires a closely related task with a large labeled data set, such as ILSVRC. An alternative

strategy is to use *companion* objective functions at each hidden layer, as a form of regularization during training [16, 15]. However, this may in principle interfere with the deep network’s ability to learn the optimal internal representations, as noted by the authors.

We propose a novel strategy for addressing the challenge of training deep CNNs given limited training data. Similar in spirit to [9, 16], we employ greedy supervised pre-training, yet in a complementary model, namely the popular Auto-context model. We then map the resulting Auto-context model onto a deep CNN, and refine all weights using back-propagation.

3 Method

In Section 3.1, we review the algorithm for mapping an RF onto an NN with two hidden layers [24, 28]. In Section 3.2, we discuss the relationship between RFs with contextual features and CNNs. In Section 3.3, we describe our first main contribution, namely how to map a cascade of RFs onto a deep CNN. In Section 3.4, we describe our second main contribution, namely an algorithm for mapping our deep CNN back onto the original RF cascade, with updated parameters.

3.1 Mapping a Random Forest to a Neural Network with Two Hidden Layers

A decision tree consists of a set of split nodes, $n \in \mathcal{N}^{Split}$, and leaf nodes, $l \in \mathcal{N}^{Leaf}$. Each split node n processes the subset X_n of the feature space X that reaches it. Usually, $X = \mathbb{R}^F$, where F is the number of features. Let $cl(n)$ and $cr(n)$ denote the left and right *child node* of a split node n . A split node n partitions the set X_n into two sets $X_{cl(n)}$ and $X_{cr(n)}$ by means of a *split decision*. For DTs using axis-aligned split decisions, the split is performed on the basis of a single feature whose index we denote by $f(n)$, and a respective threshold denoted as $\theta(n)$: $\forall \mathbf{x} \in X_n : \mathbf{x} \in X_{cl(n)} \iff x_{f(n)} < \theta(n)$.

For each leaf node l , there exists a unique path from root node n_0 to leaf l , $P(l) = \{n_i\}_{i=0}^d$, with $n_0 \dots n_d \in \mathcal{N}^{Split}$ and $X_l \subseteq X_{n_d} \subseteq \dots \subseteq X_{n_0}$. Thus, leaf membership can be expressed as follows:

$$\mathbf{x} \in X_l \iff \forall n \in P(l) : \begin{cases} x_{f(n)} < \theta(n) & \text{if } X_l \subseteq X_{cl(n)}. \\ x_{f(n)} \geq \theta(n) & \text{if } X_l \subseteq X_{cr(n)}. \end{cases} \quad (1)$$

Each leaf node l stores votes for the semantic class labels, $\mathbf{y}^l = (y_1^l \dots y_C^l)$, where C is the number of classes. For a feature vector \mathbf{x} , we denote the unique leaf of the tree that has $\mathbf{x} \in X_l$ as $\text{leaf}(\mathbf{x})$. The prediction of a DT for feature vector \mathbf{x} to be of class c is given by:

$$p(c|\mathbf{x}) = \frac{y_c^{\text{leaf}(\mathbf{x})}}{\sum_{c=1}^C y_c^{\text{leaf}(\mathbf{x})}} \quad (2)$$

Using this notation, we now describe how to map a DT to a feed-forward NN, with two hidden layers.

Hidden Layer 1. Conceptually, the NN separates the task of evaluating the split nodes and evaluating leaf membership into the first and second hidden layers, respectively (see Figure 2(a,b)). Thus, the first hidden layer, H_1 , is constructed with one neuron, $H_1(n)$, per split node in the corresponding DT. This neuron evaluates $x_{f(n)} \geq \theta(n)$, and encodes the outcome in its activity, $a(H_1(n))$. H_1 is connected to the input layer with the following weights and biases: $w_{f(n), H_1(n)} = str_{01}$ and $b_{H_1(n)} = -str_{01} \cdot \theta(n)$. The global constant str_{01} sets how rapidly the neuron activation changes as its input crosses its threshold. All other weights in this layer are zero.

Concerning the activation function in H_1 , $a(\cdot) = \tanh(\cdot)$ is used, with a large value for str_{01} to approximate thresholded split decisions. During training, str_{01} can be reduced to avoid the problem of diminishing gradients in back-propagation; however, for now we assume str_{01} is a large positive constant. Thus, for each node n and feature vector $\mathbf{x} \in X_n$ the following holds: $\mathbf{x} \in X_{cl(n)} \iff a(H_1(n)) = -1$. The pattern of activations encodes leaf node membership as follows:

$$\mathbf{x} \in X_l \iff \forall n \in P(l) : \begin{cases} a(H_1(n)) = -1, & \text{if } X_l \subseteq X_{cl(n)}. \\ a(H_1(n)) = +1, & \text{if } X_l \subseteq X_{cr(n)}. \end{cases} \quad (3)$$

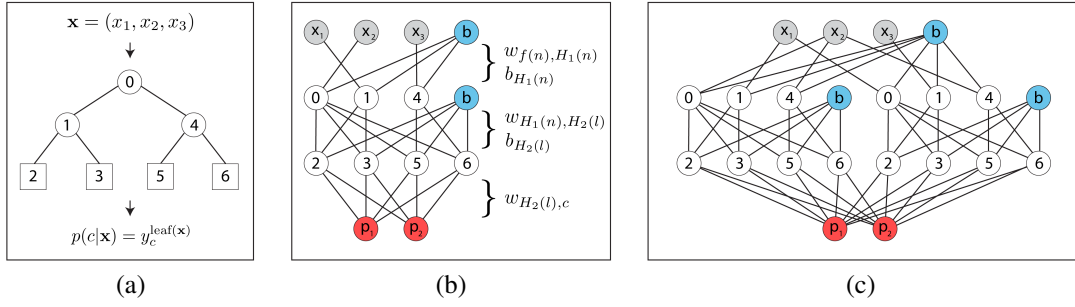


Figure 2: **Mapping from a RF to a NN.** (a) A shallow DT. Nodes are labeled to show mapping to NN. (b) Corresponding NN with two hidden layers. The first hidden layer is connected to the input layer through weights $w_{f^{(n)}, H_1^{(n)}}$, and encodes the results of feature tests evaluated for each split node of the DT (numbered 0,1,4). The weights $w_{H_1^{(n)}, H_2^{(l)}}$ between the two hidden layers encode the structure of the tree. In particular, the split nodes along the path $P(l)$ are connected to $H_2^{(l)}$. For example, leaf node 5 is connected to split node 0, but not split node 1. The second hidden layer encodes leaf membership for each leaf node (numbered 2,3,5,6). The final weights $w_{H_2^{(l)}, c}$ are fully connected and store the votes y_c^l for each leaf l and class c . Gray: Input feature nodes. Blue: Bias nodes. Red: Prediction nodes, $p(c|\mathbf{x})$. (c) NN corresponding to a RF with two DTs, each with the same architecture as in (a). Note that, while the two DTs have the same architecture, they use different input features at each split node, and do not share weights.

Hidden Layer 2. The role of neurons in the second hidden layer, H_2 , is to interpret the activation pattern a feature vector \mathbf{x} triggers in H_1 , and thus identify the unique leaf $\text{leaf}(\mathbf{x})$. Therefore, for every leaf l in the DT, one neuron is created, denoted as $H_2(l)$. Each such neuron is connected to all $H_1^{(n)}$ with $n \in P(l)$, but no others. Weights are set as follows: $w_{H_1^{(n)}, H_2^{(l)}} = -str_{12}$ if $X_l \subseteq X_{cl^{(n)}}$ and $w_{H_1^{(n)}, H_2^{(l)}} = +str_{12}$ if $X_l \subseteq X_{cr^{(n)}}$. The sign of these weights matches the pattern of incoming activations iff $\mathbf{x} \in X_l$, thus making the activation of $H_2(l)$ maximal. To distinguish leaf membership, the biases in H_2 are set as $b_{H_2^{(l)}} = -str_{12} \cdot (|P(l)| - 1)$. Thus the input to node $H_2(l)$ is equal to 1 if $\mathbf{x} \in X_l$, and less than or equal to -1 otherwise. Using tanh activation functions, linearly scaled to $[0, 1]$ range, and a large value for str_{12} , the neurons approximately behave as binary switches that indicate leaf membership. *I.e.*, $a(H_2(\text{leaf}(\mathbf{x}))) = 1$ and all other neurons are silent.

Output Layer. The output layer of the NN has C neurons, one for every class label. This layer is fully connected; however, there are no bias nodes introduced. The weights store scaled votes from the leaves of the corresponding DT: $w_{H_2^{(l)}, c} = str_{23} \cdot y_c^l$. A softmax activation function is applied, to ensure a probabilistic interpretation of the output after training:

$$p(c|\mathbf{x}) = \frac{\exp(str_{23} \cdot y_c^{\text{leaf}(\mathbf{x})})}{\sum_{c=1}^C \exp(str_{23} \cdot y_c^{\text{leaf}(\mathbf{x})})} \quad (4)$$

Note that the softmax activation slightly perturbs the output distribution of the original RF (cf. Equation 2), making the mapping approximate. This can be tuned by the choice of str_{23} , and in practice is a minor effect. Importantly, the softmax activation preserves the MAP solution.

From a Tree to a Forest. An RF is a collection of DTs. Let the number of DTs in a forest be denoted as T . The prediction of a forest for feature vector \mathbf{x} to be of class c is the normalised sum over the votes stored in the single leaf per tree t , denoted $\text{leaf}_t(\mathbf{x})$:

$$p(c|\mathbf{x}) = \frac{\sum_{t=1}^T y_c^{\text{leaf}_t(\mathbf{x})}}{\sum_{c=1}^C \sum_{t=1}^T y_c^{\text{leaf}_t(\mathbf{x})}} \quad (5)$$

Extending the DT-to-NN mapping described above to RFs is trivial: (i) replicate the basic NN design T number of times, and (ii) fully connect H_2 to the output layer (see Figure 2(c)). This accomplishes summing over the leaf distributions from the different trees, before the softmax activation is applied.

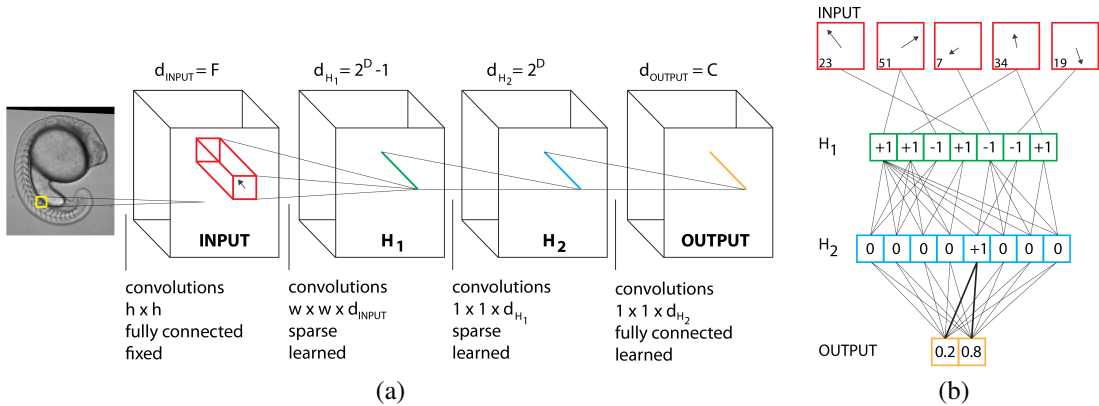


Figure 3: **CNN architecture of a RF.** (a) CNN architecture for dense semantic segmentation, corresponding to a RF with contextual features. Note there are no max pooling layers in this CNN architecture. The variables are: h - size of input convolution kernels; F - number of input convolution kernels; w - window size for offset features; d - number of feature maps in each layer; D - depth of corresponding decision tree; C - number of classes. (b) An example, where the RF is a single DT with depth $D = 3$, and 2 output classes. One pixel is classified in (b), corresponding to the region in (a) with similar color-coding. The input layer (red) extracts features with a fixed offset (shown by arrows) and filter type (index into filter stack, shown at bottom left of each node). Activation values are shown for nodes in H_1 , H_2 and the output layer. In this example, $\text{leaf}(\mathbf{x}) = 5$, highlighted by bold edges leading to the output layer. Bias nodes not shown for simplicity.

3.2 Relationship Between Random Forests and Convolutional Neural Networks

One of the defining characteristics of CNNs is weight sharing across neurons corresponding to the same feature map. These neurons compute convolutions over a local window in their input, and their convolutional weights are constant across the entire feature map. Unsurprisingly, RFs work in the same way. A feature vector is pre-computed for each pixel in the image, and then fed through the same forest, or in the NN formulation given above, it traverses the identical NN. There are however some key differences. In a RF, the first “convolutional layer” is pre-computed with a hand-selected filter bank, not learned as in a CNN. The subsequent operations of the RF can be broken down into two convolutions (corresponding to H_1 and H_2) each with height and width 1. The first of these two convolutions has depth equal to the number of filters in the filter bank, denoted F (typically 10 – 1000s), and is very sparse. E.g., axis-aligned decision stumps correspond to a convolution kernel with only a single non-zero element. The second convolution (H_2) is similarly very sparse, with the number of non-zero elements equal to the depth of the tree. Recall from 3.1, each neuron $H_2(l)$ in this layer combines the response of all split node neurons along path $P(l)$.

In many applications such as scene labeling [27], body-pose estimation [21], and medical image labeling [18], contextual information is included in the form of “offset features” that are selected from within a window defined by a maximum offset, Δ_{max} . Thus, neurons in H_1 compute sparse convolutions with width $w = 2 * \Delta_{max} + 1$, and depth F . Again, it is conventional to have only a single non-zero element in this convolution kernel; however, in the case of medical imaging it is also common to use average intensity over an offset window [18]. Clearly, sparsity is very important, otherwise the convolutional kernel could easily have as many as 10^6 elements. A RF approaches this task by generating a large number of sparse convolutions. E.g., for a balanced tree of depth 10, H_1 creates 1023 feature maps, where each neuron has a single input. H_2 creates 1024 feature maps, but each neuron combines 10 features from the previous layer. Thus, a RF with contextual features can be viewed as a special case of a CNN, with sparse convolutional kernels and no max pooling layers (See Figure 3 for a schematic of the CNN architecture). As we shall see in the next section, cascaded RFs simply iterate this architecture using the previous RF predictions as input features, thereby generating a deep CNN.

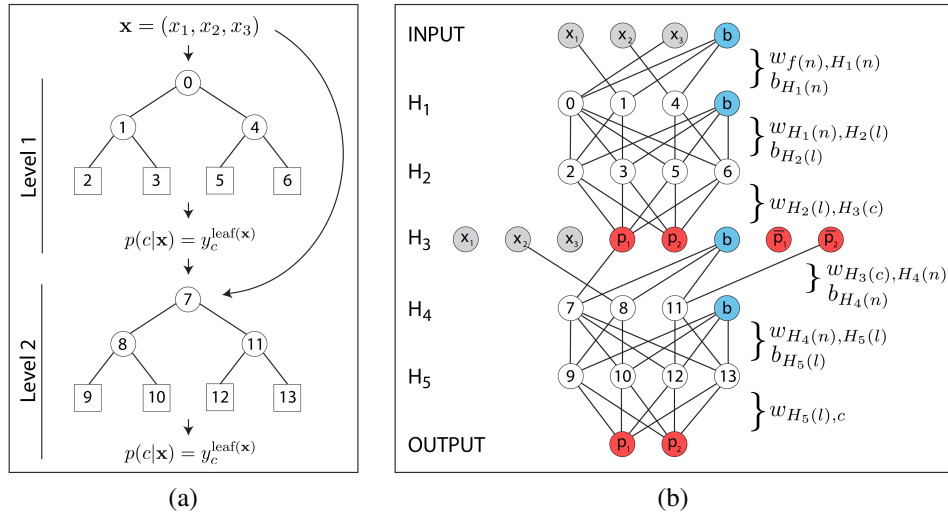


Figure 4: **Mapping from a cascaded RF to a deep CNN.** (a) A cascaded RF consisting of 2 shallow decision trees. The second RF takes as input the set of convolutional filter responses, and the output of the previous RF. (b) Corresponding CNN with 5 hidden layers. Same color coding and node labeling as in Figure 2. In this example, the second DT learned to use filter response x_2 , the RF output for class 1 at that pixel (*i.e.* p_1), and the RF output for class 2 at some different offset pixel, denoted \bar{p}_2 . Note: \bar{p}_2 is not a bias node; its value depends on weights in previous layers.

3.3 Mapping a Random Forest Cascade to a Deep Convolutional Neural Network

In a cascade of RFs, the modular architecture of a single RF is repeated. We map this architecture onto a deep CNN as follows: Each RF is mapped to a CNN, and then these CNNs are concatenated such that the layers corresponding to intermediate RF predictions become hidden layers, used as input to the next CNN in the sequence (see Figure 4). For a K -level RF cascade, this generates a deep CNN with $3K - 1$ hidden layers. In the original Auto-context algorithm [27], each classifier can either select a feature from the output of the previous classifier, or from the set of input filter responses. Thus, we also introduce the input filter responses as bias nodes in hidden layers H_{3k} , $k = 1 \dots K - 1$. We note that both addition of trees to the RF and/or growing trees to a greater depth results in a CNN with 2 hidden layers, but with greater width. However, cascading RFs naturally increases the depth of the CNN architecture.

An interesting question is what activation function to use on layers H_{3k} , which are no longer prediction layers. We explored the following options: identity, tanh, class normalization, and softmax. Despite the fact that class normalization can in principle become undefined, due to the possibility of having negative weights, we found that it out-performed the other options. In particular, softmax was the most problematic, because it perturbs the prediction with regards to the original RF, and this error is compounded in a deep cascade. This is consistent with class normalization performing the best, since it exactly matches the operation in the original RF cascade (cf. Equation 5). For the rest of the paper, we use class normalization activation functions on layers H_{3k} . We apply softmax activation at the final output layer.

In cascaded RFs used for semantic segmentation, individual pixels cannot be run through the entire cascade independently, but rather the complete image must be run through one level at a time, such that all features are available for the next level. This is similarly true for our deep CNN.

3.4 Mapping the Deep Convolutional Neural Network back to a Random Forest Cascade

We are interested in mapping our deep CNN architecture back to a cascaded RF, with axis-aligned split functions, for fast evaluation at test time. Given a CNN constructed from a K -level RF cascade as described above, the weights $w_{H_{3k-2}, 3k-1}$, $k = 1 \dots K$ manifest the correspondence of the CNN with the original tree structure. Thus, during training, keeping these weights and the corresponding biases, $b_{H_{3k-1}}$ fixed, allows the CNN to be trivially mapped back to the original RF cascade. For

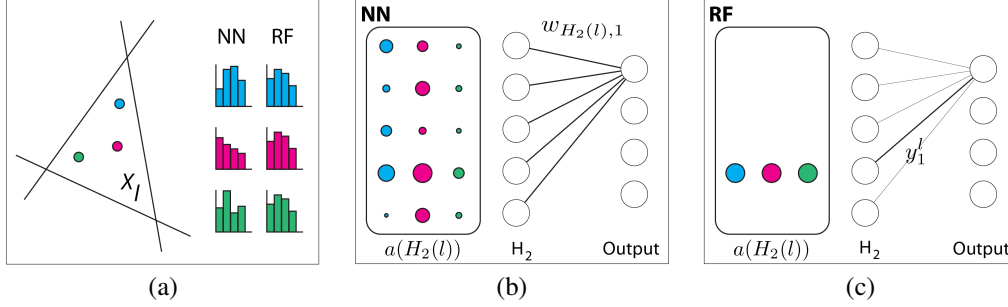


Figure 5: **Mapping CNN back to a RF.** (a) Three samples (blue, magenta, green) falling into the leaf of a DT, corresponding to a subset X_l of feature space, have the same posterior distributions; however, in a CNN their posteriors can be different. (b) Corresponding activation pattern $a(H_2(l))$ for the three samples shown in (a) at H_2 of RF initialized NN. The output layer receives the inner product of the activation pattern with weights $w_{H_2(l),c}$ (only weights to class 1 shown with black line). (c) Activation pattern in corresponding RF. Note, the inner product reduces to the value y_1^l for class 1.

a single level cascade, the mapping is: (i) $\theta(n) = -b_{H_1(n)}/w_{f(n),H_1(n)}$, (ii) $y_c^l = w_{H_2(l),c}$. We refer to this as “Map Back #1”. Finally, when evaluating this RF, a softmax activation function needs to be applied to the output distribution. For deeper cascades, the output of *each* RF must be post-processed with the corresponding activation function in the CNN, which in this paper is simple class normalization, but could be something different, such as softmax.

While the approach described above does map the CNN architecture back to the original RF Cascade, it may not make optimal use of the parameter refinement learned during back-propagation. Above, for a single level cascade we assigned $y_c^l = w_{H_2(l),c}$, which is the correct thing to do if only a single leaf neuron $H_2(l)$ fires in the network. However, after training by back-propagation, the activation pattern in H_2 may be distributed, with many neurons contributing to the prediction.

Here, we propose a strategy to capture the distributed activation of the CNN by updating the votes stored in the RF leaves. For feature vector \mathbf{x} and class c , we would ideally like to store in $\text{leaf}_l(\mathbf{x})$, the inner product of the activation pattern in H_2 with the out-going weights:

$$z_{\mathbf{x}}(c) := \sum_{l \in \mathcal{N}^{Leafs}} a_{\mathbf{x}}(H_2(l)) \cdot w_{H_2(l),c}. \quad (6)$$

This would elicit the identical output from the RF as from the CNN for input \mathbf{x} . However, the activation pattern will vary for different training samples that end up in the same leaf, so this mapping cannot be satisfied simultaneously for the whole training set. In other words, DTs store distributions in their leaves l that represent constant functions on the respective X_l , while the re-trained CNN allows for non-constant functions on X_l (see Figure 5). As a compromise, we seek new vote distributions \hat{y}_c^l , for each c, l , to minimise the following error, averaged over the finite set of training samples, $X^{\text{train}} \subset X$.

$$\sum_{\mathbf{x} \in X^{\text{train}}: \text{leaf}(\mathbf{x})=l} (z_{\mathbf{x}}(c) - \hat{y}_c^l)^2 \quad (7)$$

Equation 7 can be solved analytically, yielding the following result:

$$\hat{y}_c^l = \frac{1}{|\{\mathbf{x} \in X^{\text{train}} : \text{leaf}(\mathbf{x}) = l\}|} \sum_{\mathbf{x} \in X^{\text{train}}: \text{leaf}(\mathbf{x})=l} z_{\mathbf{x}}(c) \quad (8)$$

This is a simple average of $z_{\mathbf{x}}(c)$ over all samples that end up in the same leaf of the corresponding DT. We refer to this as “Map Back #2”. In the trivial case where, for every sample, only one neuron fires in H_2 , this is equivalent to “Map Back #1”.

To implement this algorithm in a cascade, we must take one additional precaution. Since updating the votes as described in Equation 8 does not capture the output of the re-trained CNN exactly, we update

the votes sequentially, from the first to the last level of the corresponding cascade. *E.g.*, for a 2 level cascade, after updating the votes in the first RF using Equation 8, we pass the training data through and determine the new value of $\text{leaf}(\mathbf{x})$ in the second RF for each training sample, and use this to update the votes in the second RF. See Algorithm 1 for details.

Algorithm 1 Algorithm for mapping deep CNN back to K-level RF cascade

1. Push all training data through CNN
 2. Store $a_{\mathbf{x}}(H_{3k-1}(l))$, for $k = 1 \dots K$
- for** $i = 1 : K$ **do**
- Push all training data through RF cascade, up to level i
 - Store $\text{leaf}_i(\mathbf{x})$, at level i
 - Update votes in i^{th} RF to \hat{y}_c^l , according to Eq. 8
- end for**
-

4 Results and Discussion

Experimental Setup. We applied our method to semantic segmentation of 21 somites and 1 background class in a data set of 32 images of developing zebrafish, with a resolution of 800 x 950 pixels. Experts in biology manually created ground truth segmentations of these images. This data set poses multiple challenges for automated segmentation, due to the similar appearance of neighboring segments and the limited training data. The data set was split into 16 images for training and 16 images for test. We evaluated resulting segmentation on the test images by means of the Dice score averaged over all 21 foreground classes.

Cascaded Random Forest. We trained a three-level RF cascade, with the following forest parameters at every level: 16 trees, maximum depth 12, stop node splitting if less than 25 samples. Features were extracted from the images using a standard filter bank, and then normalized to zero mean, unit variance. The number of random features tested in each node was set to the square root of the feature dimension. For each randomly selected feature, 10 additional contextual features were also considered, with X and Y offsets within a 129x129 pixel window. 2 additional training images were generated per original training image by random rotation of the originals, with uniform probability over the range [-10,10] degrees. Training samples were generated by sub-sampling the training images 3x in each dimension and then randomly selecting 25% of these samples for training.

Segmentation of the test data by means of the resulting cascaded RF achieved an average Dice score of 0.60 (see Figure 6(c) and Table 1(RF Cascade)).

Improving Cascaded Random Forests by Training in a Deep Neural Network Architecture. We map the RF cascade to a deep CNN with 8 hidden layers, as described in Section 3. For efficient training, the initialization parameters $str_{01} - str_{89}$ were reduced such that the network transmits a strong gradient via back-propagation. However, softening these parameters moves the deep CNN further from its initialization by the equivalent cascaded RF. We evaluated a range of initialization parameters and found $str_{01} = str_{34} = str_{67} = 100$, $str_{12} = str_{45} = str_{78} = 1$, $str_{23} = str_{56} = str_{89} = 0.1$ to be a good compromise.

We trained the CNN using back-propagation and stochastic gradient descent (SGD), with a cross-entropy loss function. During back-propagation, we maintained the sparse connectivity from RF initialization, allowing only the weights on pre-existing edges to change, corresponding to the *sparse* training scheme from [28]. SGD training is applied by passing images through the network one at a time, and computing the gradient averaged over all pixels (*i.e.*, batch size = 1 image). Thus, we do “whole-image-at-a-time” training, as in [17]. Training samples were generated by sub-sampling the training images 9x in each dimension. Learning rate, r , was optimized for network performance and set such that for the i^{th} iteration of SGD, $r(i) = a(1 + i/b)^{-1}$ with hyper-parameters $a = 0.01$ and $b = 96$ iterations. Momentum was initialized to 0.4, and increased to 0.7 after 96 iterations. We observed convergence after only 1-2 passes through the training data, similar to what was reported by [11]. Using this strategy, we achieved a Dice score of 0.66, corresponding do a 10% relative improvement over the RF cascade (see Figure 6(d) and Table 1(Deep CNN)).

The architecture of the deep CNN preserves the intermediate prediction layers of the RF cascade, which generates one image for each class at the same resolution as the input image. However, due to

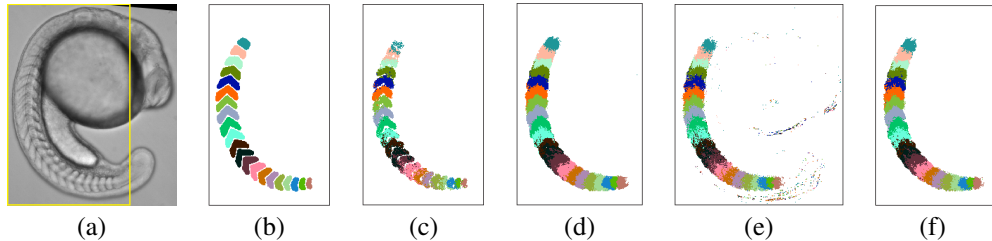


Figure 6: **Comparison of different methods.** (a) Raw image of zebrafish. Yellow box denotes crop for b,c,d,f. (b) Expert ground truth labeling. (c) Prediction of cascaded RF. (d) Prediction of corresponding deep CNN, after parameter refinement. (e) Prediction of “Map Back #1” RF Cascade. (f) Prediction of “Map Back #2” RF Cascade. See Section 3.4 for details of map back algorithms.

Level	Dice Score			
	RF Cascade	Deep CNN	Map Back #1	Map Back #2
1	0.37	-	-	-
2	0.49	-	-	-
3	0.60	0.66	0.59	0.63

Table 1: **Dice score of dense semantic labeling by different methods.** Dice score is reported after each level in the RF cascade, and after the final prediction in the deep CNN. See Section 3.4 for details of map back algorithms.

back-propagation training, these images no longer represent probability distributions. In particular, the pixel values can now be negative. We visualized the internal layers to better understand how they changed during additional training in the CNN (Figure 7). First, we observed that at each level, the intermediate prediction layer is perturbed with regards to the equivalent layer in the RF cascade, implying that the back-propagation training permeated the deep network. Interestingly, we also noticed that the internal activation layers were much smoother in the CNN. A common strategy in cascaded classification is to introduce smoothing between the layers of the cascade (see *e.g.* [13, 12, 22]). It appears that a similar strategy is naturally learned by the deep CNN, which tends to smooth the class probabilities along the direction of other foreground classes.

Mapping the trained CNN back to a cascaded RF. We first evaluated the trivial approach of mapping weights directly onto votes, similar to what was done in the RF to NN mapping; however, this reduced the Dice score to 0.59 (see Figure 6(e) and Table 1(Map Back #1)), worse than the performance of the initial RF. Next we applied Algorithm 1, which produces a result that is visually superior to the trivial mapping, and yields a final Dice score of 0.63 (see Figure 6(f) and Table 1(Map Back #2)). Thus, we achieve a 5% relative improvement of our RF cascade, which retains its exact tree structure, by mapping to a deep CNN, training all weights by back-propagation, and mapping back to the original RF cascade with updated threshold and leaf distributions.

Training Deep Neural Networks on Small Training Sets. Above we described a method for training a deep CNN on relatively little training data, using a novel initialization from a cascaded RF. As a comparison, we considered the task of training the same CNN architecture from a random initialization. We applied a similar SGD training routine, and re-tuned the hyper-parameters as follows: $a = 3 * 10^{-5}$, $b = 96$ iterations, momentum initialized to 0.4 and increased to 0.99 after 96 iterations. Networks were trained for 2500 iterations.

We first attempted to train the network maintaining the sparsity of the weight layers. However, the energy quickly plateaued, and yielded a final Dice score of only 0.04. We then fully connected the layers corresponding to the tree connectivity, (*i.e.* $w_{H_1(n), H_2(l)}, w_{H_4(n), H_5(l)}, w_{H_7(n), H_8(l)}$) and retrained with the same hyper-parameters. This network performed considerably better, reaching a final Dice score of 0.15. It is possible that this network would further improve given a better choice of hyper-parameters. However, the fully connected network has on the order of 50 million parameters, and our training uses less than 1 million pixels, which could easily lead to over-fitting.

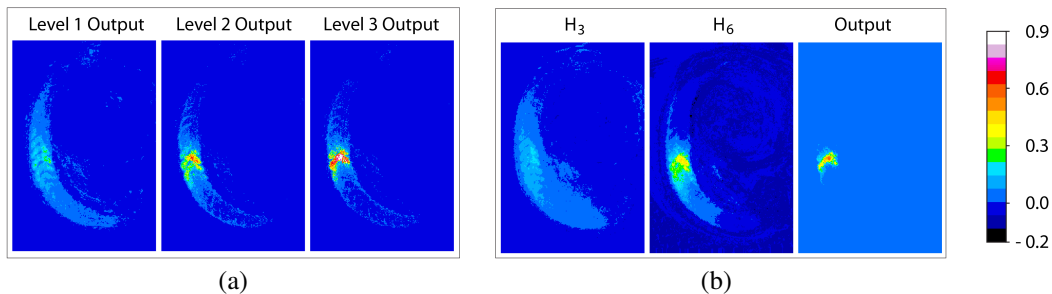


Figure 7: **Visualization of internal activation layers.** Intermediate layers corresponding to class 8 are visualized for the (a) cascaded RF and (b) deep CNN. Interestingly, the activation from the CNN appears smoothed along the direction of the foreground classes compared to the noisier output of the cascaded RF. Best viewed in colour.

In the future, it would be interesting to compare our result to other network architectures, such as a Fully Convolutional Network [17] that has been pre-trained on a large training set and then retrained on our small training set. However, this is beyond the scope of the paper.

5 Conclusion and Future Work

We describe a method for constructing a deep CNN from a pre-trained cascaded RF. This generates a novel CNN architecture that is learned from the data, with pre-initialized weights. This architecture is naturally suited to the task of semantic segmentation, and generates internal activation images, one for each class, of the same dimension as the input image. This has the added benefit that network behaviour can be directly visualized, and differentiable models can, in principle, be included as layers in the CNN that act directly on these images. Furthermore, we demonstrate that the performance of the RF cascade can be improved upon using conventional tools such as back-propagation. By visualizing the internal activation images, we observe that the network learns to smooth the intermediate probability maps with respect to the greedily trained RF Cascade. Finally, we develop an algorithm for mapping the CNN back onto the RF cascade with new thresholds and leaf distributions, for efficient evaluation at test time. There are many avenues for future work. One immediate next step is to refine the input convolution filters, which are currently fixed, during back-propagation.

References

- [1] Amr Ahmed, Kai Yu, Wei Xu, Yihong Gong, and Eric Xing. Training Hierarchical Feed-Forward Visual Recognition Models Using Transfer Learning from Pseudo-Tasks. In *ECCV*, 2008.
- [2] Yoshua Bengio. Practical Recommendations for Gradient-Based Training of Deep Architectures. In *Neural Networks: Tricks of the Trade*, pages 437–478. 2012.
- [3] Leon Bottou. Stochastic gradient descent tricks. In *Neural Networks: Tricks of the Trade*, pages 421–436. 2012.
- [4] Leo Breiman. Random forests. *Machine Learning*, 45(1):5–32, 2001.
- [5] Samuel Rota Bulò and Peter Kotschieder. Neural decision forests for semantic image labelling. In *CVPR*, 2014.
- [6] Liang-Chieh Chen, George Papandreou, Iasonas Kokkinos, Kevin Murphy, and Alan L Yuille. Semantic Image Segmentation with Deep Convolutional Nets and Fully Connected CRFs. In *ICLR*, 2015.
- [7] Dan Ciresan, Alessandro Giusti, Luca M Gambardella, and Jürgen Schmidhuber. Deep Neural Networks Segment Neuronal Membranes in Electron Microscopy Images. In *NIPS*, 2012.
- [8] Alexey Dosovitskiy, Jost Tobias Springenberg, Martin Riedmiller, and Thomas Brox. Discriminative unsupervised feature learning with convolutional neural networks. In *NIPS*, 2014.
- [9] Scott Fahlman and Christian Lebiere. The Cascade-Correlation Learning Architecture. In *NIPS*, 1990.
- [10] Clement Farabet, Camille Couprie, Laurent Najman, and Yann LeCun. Learning Hierarchical Features for Scene Labeling. *PAMI*, 35(8):1915–1929, 2013.
- [11] Ross B. Girshick, Jeff Donahue, Trevor Darrell, and Jitendra Malik. Rich feature hierarchies for accurate object detection and semantic segmentation. In *CVPR*, 2014.

- [12] Varun Jampani, Raghudeep Gadde, and Peter V Gehler. Efficient facade segmentation using auto-context. In *WACV*, 2015.
- [13] Peter Kotschieder, Pushmeet Kohli, Jamie Shotton, and Antonio Criminisi. Geof: Geodesic forests for learning coupled predictors. In *CVPR*, 2013.
- [14] Alex Krizhevsky, Ilya Sutskever, and Geoffrey E. Hinton. Imagenet classification with deep convolutional neural networks. In *NIPS*, 2012.
- [15] Chen Yu Lee, Saining Xie, Patrick Gallagher, Zhengyou Zhang, and Zhuowen Tu. Deeply-supervised nets. In *AISTATS*, 2015.
- [16] R Lengelle and T Denoex. Training MLPs layer by layer using an objective function for internal representations. *Neural networks*, 9(1):83–97, 1996.
- [17] Jonathan Long, Evan Shelhamer, and Trevor Darrell. Fully convolutional networks for semantic segmentation. In *CVPR*, 2015.
- [18] A Montillo, J Tu, J Shotton, J Winn, JE Iglesias, DN Metaxas, and A Criminisi. Entanglement and differentiable information gain maximization. In *Decision Forests for Computer Vision and Medical Image Analysis*. 2013.
- [19] Feng Ning, Damien Delhomme, Yann LeCun, Fabio Piano, Leon Bottou, and Paolo Emilio Barbano. Toward automatic phenotyping of developing embryos from videos. *IEEE transactions on image processing*, 14(9):1360–1371, 2005.
- [20] Marc Aurelio Ranzato, Fu Jie Huang, Y-Lan Boureau, and Yann LeCun. Unsupervised Learning of Invariant Feature Hierarchies with Applications to Object Recognition. In *CVPR*, 2007.
- [21] Shaoqing Ren, Xudong Cao, Yichen Wei, and Jian Sun. Global refinement of random forest. In *CVPR*, 2015.
- [22] David L Richmond, Dagmar Kainmueller, Ben Glocker, Carsten Rother, and Eugene W Myers. Uncertainty-driven Forest Predictors for Vertebra Localization and Segmentation. In *MICCAI*, 2015.
- [23] Pierre Sermanet, Koray Kavukcuoglu, Sandhya Chintala, and Yann LeCun. Pedestrian Detection with Unsupervised Multi-stage Feature Learning. In *CVPR*, 2013.
- [24] Ishwar Sethi. Entropy nets: from decision trees to neural networks. *Proceedings of the IEEE*, 78(10):1605–1613, 1990.
- [25] Jamie Shotton, Matthew Johnson, and Roberto Cipolla. Semantic texton forests for image categorization and segmentation. In *CVPR*, 2008.
- [26] Alberto Suresz and James Lutsko. Globally optimal fuzzy decision trees for classification and regression. *PAMI*, 21(12):1297–1311, 1999.
- [27] Zhuowen Tu and Xiang Bai. Auto-context and its application to high-level vision tasks and 3d brain image segmentation. *PAMI*, 32(10):1744–1757, 2010.
- [28] Johannes Welbl. Casting random forests as artificial neural networks (and profiting from it). In *GCPR*, 2014.
- [29] Shuai Zheng, Sadeep Jayasumana, Bernardino Romera-Paredes, Vibhav Vineet, Zhizhong Su, Dalong Du, Chang Huang, and Philip H S Torr. Conditional Random Fields as Recurrent Neural Networks. *arXiv.org*, 2015.